

The Deflection of the Column-mounted Jib Crane with Tapered Boom by Finite Difference Method

Nebojša B. Zdravković^{1*}, Boris Jerman², Mile Savković¹, Goran Marković¹,
Marko Todorović¹, Goran Pavlović³

¹ Faculty of Mechanical and Civil Engineering in Kraljevo, University of Kragujevac, SERBIA

² University of Ljubljana, Faculty of Mechanical Engineering (FME), SLOVENIA

³ Faculty of Electronic Engineering, University of Niš, SERBIA

One of the most frequently utilized crane types in industrial applications is the column-mounted jib crane. There are many different designs according to different requirements about lifting height, span, payload capacity, drive options, etc. Within the efforts to optimize the structure's mass, heavy-duty jib cranes with high payload capacity and extended reach often have their boom tapered. Besides strength, deflection is the most considered design criteria, where the crane structure is subjected to the total payload capacity at the tip of the boom. The paper presents the application of the finite difference method (FDM) and MATLAB code for the deflection of the column-mounted jib crane with a tapered boom. Obtained results are very close to the results from the finite element method (FEM) model in Ansys.

Keywords: Jib crane, Tapered boom, Deflection, Finite difference method.

1. INTRODUCTION

Jib cranes are one of the most commonly installed crane types in industrial facilities. They are used for frequent load handling within a circular working space. They are suitable for applications requiring repetitive lifting and transferring of loads. The column-mounted jib crane is a piece of highly efficient hoisting equipment. It requires a small space for installation, and it is very safe, energy-efficient and easy to control during operation. The payload capacity usually goes up to 5 tons, while the reach usually goes up to 6 meters.

An adequately designed jib crane should have increased the material handling efficiency and speed up the workflow. Modern industries require versatile, flexible and cost-effective material handling equipment with increased productivity. The requirements are usually related to payload capacity, span/reach, lifting height, drive options, etc. Therefore, there are many designs of jib cranes, depending on various requirements. Nevertheless, the typical column-mounted jib crane consists of the column, the boom or the jib, the boom support leg (optionally) and the hoist mounted on the trolley, which moves along the crane boom. An essential feature of the jib crane is its static and dynamic stability, dependent on the structure's deflection.

Since the jib cranes are the most widespread in industrial facilities, many engineers tried to simplify the model and quickly define these cranes' basic parameters. FEM models of the jib cranes certainly give the results relevant for calculation and dimensioning but also require a longer time to set up the calculation model.

Usually, during the design, the maximum displacement of the jib crane boom tip is critical. So, it is important to determine a simple expression for the boom deflection, based on which it is possible to define the basic parameters of the crane. In such a way, the basic geometric parameters can be defined quickly, which would shorten the design time.

The structural analysis of the jib crane with different cross-sections was performed in the paper [01], where experimental tests and FEM were used to validate the results.

Paper [02] gives a comparative analysis of several concept solutions of jib cranes by implementing the beam, plate and volume finite elements using several software packages. Several parameters (deformation energy over construction elements, kinetic and potential energy over mode shapes of natural frequencies, etc.) were used for local elements optimization. The goal was mass reduction and the increase of the natural frequencies.

The paper [03] presented an analytical model of the lateral-torsional buckling behaviour of steel web tapered tee-section cantilevers when subjected to a uniformly distributed load and/or a concentrated load at the free end. The model check was performed through FEM.

The elastic lateral-torsional behaviour of the cantilever is analysed in [04]. The obtained results in this research can be easily applied in designing the boom of the jib crane. A parametric study is carried out to examine the effectiveness of different types of restraint, the influence of the restraint stiffness and the interplay between these two aspects and the degree of web tapering.

Paper [05] shows the stress and deflection analysis of the jib crane structure for different web thicknesses and heights. The structure locations with maximum deflection and maximum stresses were determined.

The optimization of the jib crane by the evolutionary algorithm was carried out in [06], which enabled significant material savings.

Paper [07] presents the length optimization of the boom support leg, which connects the jib with the column. The authors performed the analysis using FEM. The paper showed the influence of the leg's height on the deflection of the structure.

Based on the effect of self-weight different distribution and large deformation, a mathematical model

*Corresponding author: Dositejeva 19, 36000 Kraljevo, Serbia, zdravkovic.n@mfv.kg.ac.rs

of telescopic jib displacement was established in [08]. Authors deduced a formula of endpoint displacement of large slenderness ratio telescopic jib structure. Also, the large-deformation finite element method is used as a criterion to evaluate the correctness and precision of the theoretical calculation formula.

The stress and the deflection calculations were performed through finite element analysis (FEA) in [09]. Firstly, after using analytical expressions, the density of the mesh was corrected. In the second phase of the calculation, the height and thickness of the web were varied.

The analysis of stresses and deflections was performed by using FEA in [10]. Also, the analysis of individual parts for the connection with the fundament was carried out.

Using FEA and the direct integration method, the dynamic responses of the jib crane structure in vertical and horizontal directions were considered in [11]. Forced vibration responses of the jib structure due to equivalent moving forces were determined, where the mass matrix was time-dependent.

Integrated FEA of whole jib crane model was established in [12] and arm-side deflection formula for this type of crane structure was derived.

The paper [13] gave a refined expression for the deflection of the jib crane boom tip, taking into account the actual load position at the very end of the boom.

The paper [14] shows the finite difference method (FDM) application procedure for the deflection determination on the simple elastically restrained cantilever beam with continuously varying box-like cross-section and linear change of section height.

This research applies the previous approach for determining the deflection of the column-mounted jib crane with a tapered boom.

2. THE MATHEMATICAL MODEL BY FDM

The structures of the heavy-duty cranes are optimized to achieve lighter designs and reduce production and operational costs. The column-mounted jib cranes with high lifting capacity and long reach have optimized booms with a variable cross-section (Fig. 1 [15]).

The main parameters of the model and its cross-sections are depicted in Fig. 2, while the detailed calculation model is presented in Fig. 3.



Figure 1: Heavy-duty column-mounted jib crane with a non-uniform boom [15]

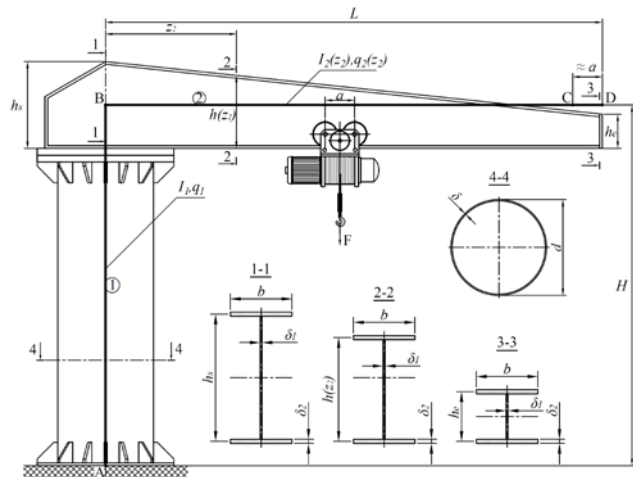


Figure 2: The model and the cross-sections

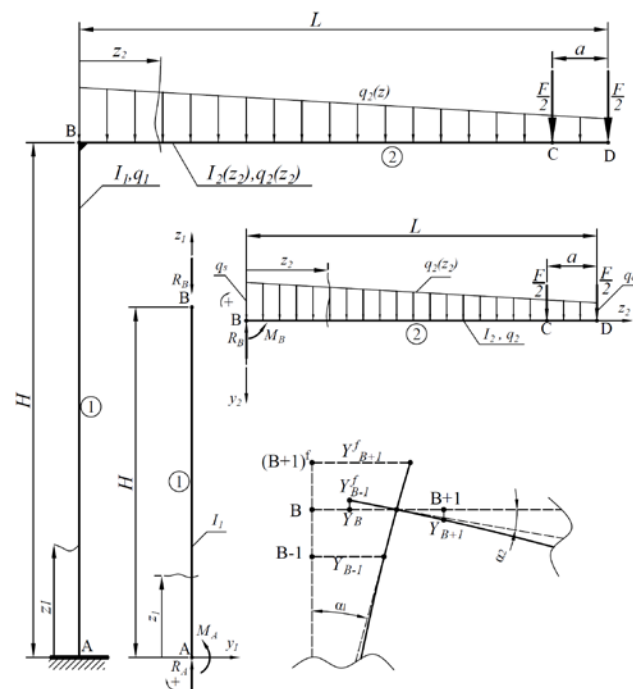


Figure 3: The calculation model with the finite difference scheme at point B

Column 1 is a thin-wall pipe with a diameter of D and wall thickness δ . The non-uniform boom 2 is a web-tapered I-beam with a linear change of its height along its longitudinal coordinate z_2 (Fig. 2). It is better to use the

distance between the flanges' centroids h than the height to simplify the expressions. In terms of the centroids' distance at the boom start (h_s) and centroids' distance at the boom tip (h_e), it has the following form:

$$h = h(z_2) = h_s - (h_s - h_e) \frac{z_2}{L} \quad (1)$$

where L – boom's length.

The web thickness is δ_1 , while the thickness of the flanges is δ_2 . The flanges of the I-beam have constant width b along the longitudinal boom axis.

Hence, the moment of inertia of web-tapered I-beam can be written as follows

$$I_2(z_2) \approx \frac{\delta_1 h^3 + 6b\delta_2 h^2}{12} \quad (2)$$

Further, the approximate but more straightforward expression for its cross-sectional area is

$$A_2(z_2) \approx 2b\delta_2 + \delta_1 h \quad (3)$$

So, the weight per unit length of the boom reads

$$q_2(z_2) \approx \rho g(2b\delta_2 + \delta_1 h) \quad (4)$$

where ρ – mass per unit volume for steel and g - gravity.

Hence, the starting and ending weight per unit length of the boom are

$$q_s = q_2(z_2 = 0) = \rho g A_2(z_2 = 0) \approx \rho g(2b\delta_2 + \delta_1 h_s)$$

$$q_e = q_2(z_2 = L) = \rho g A_2(z_2 = L) \approx \rho g(2b\delta_2 + \delta_1 h_e)$$

Static equilibrium of the structure gives the following expressions for forces and bending moments

$$R_B = F + \left(2b\delta_2 + \delta_1 \frac{h_s + h_e}{2} \right) \rho g L \quad (5)$$

$$M_B = F \left(L - \frac{a}{2} \right) + \left[(2b\delta_2 + \delta_1 h_s) \frac{L^2}{2} - \delta_1 (h_s - h_e) \frac{L^2}{3} \right] \rho g \quad (6)$$

$$R_A = R_B + q_1 H \quad (7)$$

$$M_A = M_B \quad (8)$$

where

$q_1 = \rho g A_1$ - the weight per unit length of the column

A_1 – cross-sectional area of the column

H – the theoretical height of the column (taken along its longitudinal axis from the base plate bottom to the centroid of the boom's cross-section centroid).

Governing differential equation for bending of the column is:

$$\frac{d^2 y_1(z_1)}{dz_1^2} = -\frac{M_1(z_1)}{EI_1} = -\frac{M_1(z_1)}{B_1} = -\frac{M_A}{B_1} = \frac{M_A}{B_1} \quad (9)$$

where

$B_1 = EI_1$ - column bending stiffness,

$M_1(z_1) = -M_A = \text{const.}$ - bending moment.

According to FDM, the axial coordinate becomes $z_1 = i \cdot s$ and the second derivative of the deflection line has the approximate form:

$$y_1''(z_1) \approx \frac{Y_{i-1} - 2Y_i + Y_{i+1}}{s^2} \quad (10)$$

where

i – the point ordinal,

s – the adopted distance between two adjacent nodes along the neutral axis in an undeformed state of the structure. Hence, Eq.(9) becomes transformed:

$$\frac{Y_{i-1} - 2Y_i + Y_{i+1}}{s^2} \approx \frac{M_A}{B_1} \quad (11)$$

Boundary conditions

$$y_1(z_1 = 0) = 0 \quad (12)$$

$$y_1'(z_1 = 0) = 0$$

after transformation by FDM become

$$Y_0 = 0$$

$$\frac{-Y_{i-1} + Y_{i+1}}{2s} \Big|_0 = \frac{-Y_{-1}^f + Y_1}{2s} = 0 \Rightarrow Y_{-1}^f = Y_1 \quad (13)$$

The superscript index "f" stands for the displacement of a fictitious node (the node out of the curve domain). After introducing designation for characteristic node ordinal $B = H/s$, the deflection line of the column can be represented by the following set of algebraic equations:

$$i = 0 \rightarrow 2Y_1 = \frac{M_A s^2}{B_1}$$

$$i = 1 \rightarrow -2Y_1 + Y_2 = \frac{M_A s^2}{B_1} \quad (14)$$

$$i = 2 \div B - 1 \rightarrow Y_{i-1} - 2Y_i + Y_{i+1} = \frac{M_A s^2}{B_1}$$

Governing differential equation for bending of the tapered boom is:

$$\frac{d^2 y_2(z_2)}{dz_2^2} = -\frac{M_2(z_2)}{EI_2(z_2)} \quad (15)$$

where

$$M_2(z_2) = -M_B + R_B z_2 - \rho g \left[(2b\delta_2 + \delta_1 h_s) \frac{z_2^2}{2} - \delta_1 (h_s - h_e) \frac{z_2^3}{3L} \right]$$

$$-\frac{F}{2} [z_2 - (L - a)]$$

$$I_2(z_2) = \frac{\delta_1 h^3(z_2) + 6\delta_2 h^2(z_2)}{12}$$

According to FDM, the axial coordinate becomes $z_2 = (i - B) \cdot s$ and the second derivative of the deflection line has the approximate form:

$$y_2''(z_2) \approx \frac{Y_{i-1} - 2Y_i + Y_{i+1}}{s^2} \quad (16)$$

Boundary conditions

$$y_2(z_2 = 0) = 0 \quad (17)$$

$$y_2'(z_2 = 0) = y_1'(z_1 = H)$$

after FDM transformation yield the expressions for the displacements of the fictitious nodes before and after point B (Fig. 3)

$$Y_{B+1}^f = \frac{M_A}{B_1} s^2 + 2Y_B - Y_{B-1} \quad (18)$$

$$Y_{B-1}^f = Y_{B+1} - \frac{M_A}{B_1} s^2 - 2Y_B + 2Y_{B-1}$$

Hence, the system of algebraic equations (14) now can be continued and complemented with the algebraic equations which are derived from governing differential bending equation for the boom:

$$i = B \rightarrow 2Y_{B-1} - 2Y_B + 2Y_{B+1} = \frac{M_B s^2}{E} \left[\frac{12}{\delta_1 h_s^3 + 6b\delta_2 h_s^2} + \frac{1}{I_1} \right]$$

$$i = B+1 \rightarrow -2Y_{B+1} + Y_{B+2} = P \frac{Q}{R} \quad (19)$$

$$i = B+2 \div C-1 \rightarrow Y_{i-1} - 2Y_i + Y_{i+1} = P \frac{T}{W}$$

$$i = C \div D-1 \rightarrow Y_{i-1} - 2Y_i + Y_{i+1} = P \frac{T - \frac{F}{2} [(i-B)s - (L-a)]}{W}$$

where

$$P = \frac{12s^2}{E}$$

$$Q = M_B - R_B s + \rho g \left[(2b\delta_2 + \delta_1 h_s) \frac{s^2}{2} - \delta_1 (h_s - h_e) \frac{s^3}{3L} \right]$$

$$R = \delta_1 \left[h_s - (h_s - h_e) \frac{s}{L} \right]^3 + 6b\delta_2 \left[h_s - (h_s - h_e) \frac{s}{L} \right]^2$$

$$T = M_B - R_B (i-B)s + \rho g \left[(2b\delta_2 + \delta_1 h_s) \frac{(i-B)^2 s^2}{2} - \delta_1 (h_s - h_e) \frac{(i-B)^3 s^3}{3L} \right]$$

$$W = \delta_1 \left[h_s - (h_s - h_e) \frac{(i-B)s}{L} \right]^3 + 6b\delta_2 \left[h_s - (h_s - h_e) \frac{(i-B)s}{L} \right]^2$$

$$C = \frac{H+L-a}{s}$$

$$D = \frac{H+L}{s} = N$$

3. THE COMPARISON WITH FEM MODEL RESULTS

Based on the system of algebraic equations (14) and (19), a MATLAB code was written, and the displacements for Y_j , $j=1, \dots, N=D$ nodes were calculated for the numerical example with the following data:

$E=2 \cdot 10^4 \text{ kN/cm}^2$, $H=400 \text{ cm}$, $L=600 \text{ cm}$, $F=30 \text{ kN}$, $a=80 \text{ cm}$, $d=50 \text{ cm}$, $\delta=1.2 \text{ cm}$, $b=30 \text{ cm}$, $\delta_1=1.2 \text{ cm}$, $\delta_2=1.6 \text{ cm}$.

The value of the boom's starting section height h_s was changed within interval $400 \div 600 \text{ mm}$, while its ending section height h_e took values between 200 mm and 300 mm , both incremented by a 50 mm step. The results for boom tip displacement Y_D for such input parameters are given in tables 1, 2 and 3. Also, for comparison purposes, the FEM model was built in ANSYS for each test case. The relative error is displayed in the far-right column of the tables.

Fig. 4 presents the test case in ANSYS for $h_e=200 \text{ mm}$ and $h_s=500 \text{ mm}$ (bolded cell in table 1), Fig. 5 shows the boom's tip displacement concerning the heights of the start and end section of the boom, while Fig. 6 is the graphical interpretation of results in table 1.

Table 1: Boom tip displacement for $h_e=200 \text{ mm}$

$h_e=200 \text{ mm}$			
$h_s [\text{mm}]$	$Y_D [\text{mm}]$		rel. error
	FDM	FEM	
400	69.43	71.172	-2.45%
450	63.83	65.514	-2.57%
500	59.66	61.23	-2.56%
550	56.47	57.888	-2.45%
600	53.99	55.219	-2.23%

Table 2: Boom tip displacement for $h_e=250 \text{ mm}$

$h_e=250 \text{ mm}$			
$h_s [\text{mm}]$	$Y_D [\text{mm}]$		rel. error
	FDM	FEM	
400	66.91	68.669	-2.56%
450	61.88	63.535	-2.60%
500	58.12	59.702	-2.65%
550	55.24	56.64	-2.47%
600	52.99	54.208	-2.25%

Table 3: Boom tip displacement for $h_e=300 \text{ mm}$

$h_e=300 \text{ mm}$			
$h_s [\text{mm}]$	$Y_D [\text{mm}]$		rel. error
	FDM	FEM	
400	64.9	66.665	-2.65%
450	60.32	62.029	-2.76%
500	56.89	58.476	-2.71%
550	54.25	55.684	-2.58%
600	52.19	53.427	-2.32%

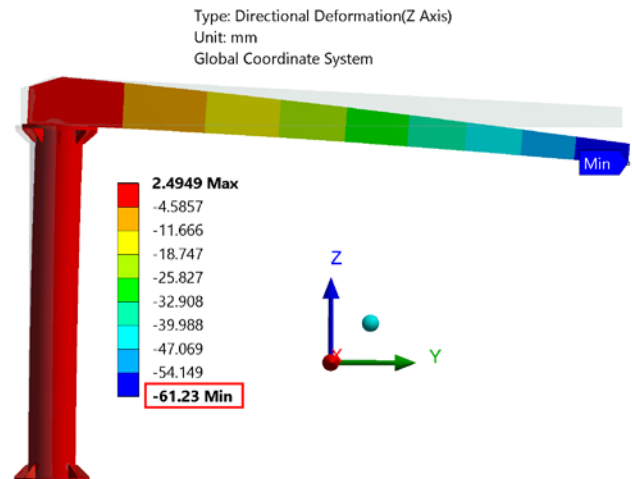


Figure 4: ANSYS test case for $h_e=200 \text{ mm}$ and $h_s=500 \text{ mm}$

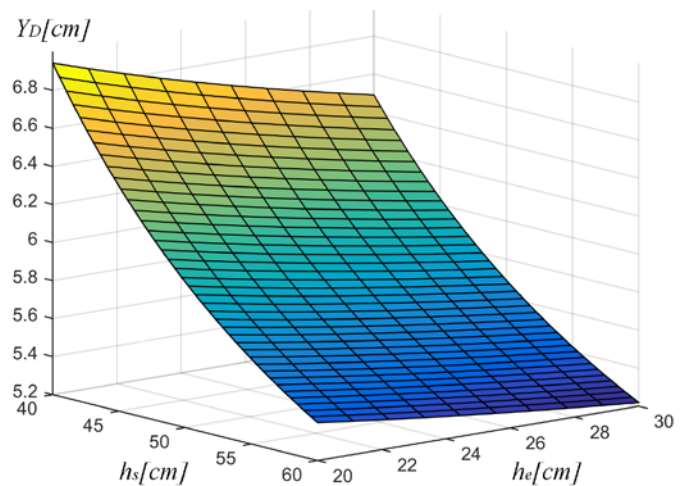


Figure 5: The boom's tip displacement in relation to its start and end section heights

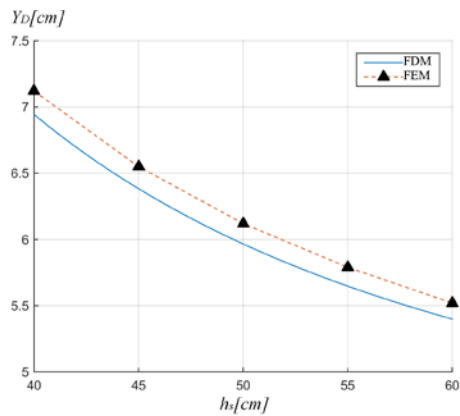


Figure 6: The graphical interpretation of results in table 1

4. THE CONCLUSION

The presented FDM method and applied algorithm yielded a compact system of algebraic equations, convenient for code writing and solving by MATLAB. The results obtained from the FDM model are in very good compliance with the results from the FEM model built in ANSYS. Relative error (less than 3%) is mainly caused by the approximate value for the boom's moment of inertia (Eq. 2). The main advantage of the FDM and the proposed procedure is that it can show the influence of any design parameter on the boom's tip displacement once written and solved, which makes it convenient for crane structure optimization. The presented FDM method is universal and can be applied to other types of cranes in the future.

ACKNOWLEDGEMENTS

This paper is supported by the Ministry of Education, Science and Technological Development of the Republic of Serbia through Contract No. 451-03-9/2021-14/200108.

REFERENCES

- [1] Chaudhary S. A., Khan N.S., "A review paper on structural analysis of cantilever beam of jib crane", *International Journal of Engineering Research and General Science*, ISSN 2091-2730, Vol. 3, No. 3, pp. 612-615, (2015)
- [2] Hadžikadunić F., Vukojević N., Huseinović S., "An analysis of jib crane constructive solution in exploitation", 12th International Research/Expert Conference "Trends in the Development of Machinery and Associated Technology" - TMT 2008, ISBN 9958-617-41-6, Istanbul, Turkey, 26–30 August 2008, pp. 789-792, (2008)
- [3] Yuan W., Kim B., Chen C., "Lateral-torsional buckling of steel web tapered tee-section cantilevers", *Journal of Constructional Steel Research*, ISSN 0143-974X, Vol 87, pp. 31-37, (2013)
- [4] Andrade A., Providência P., Camotim D., "Elastic lateral-torsional buckling of restrained web-tapered I-beams", *Computers and Structures*, ISSN 0045-7949, Vol 88, pp. 1179-1196, (2010)
- [5] Rajmane S.M., Jadhav A., "Finite element analysis of jib crane", *International journal of innovative research in technology*, ISSN 2321-1156, Volume 2, Issue 6, pp. 404-407, (2015)
- [6] Gandhare K., Thute V., "Design Optimization of Jib Crane Boom Using Evolutionary Algorithm", *International Journal of Scientific Engineering and Research (IJSER)*, ISSN Volume 3, Issue 4, pp. 5-8, (2015)
- [7] Yawale P., Khandare N., "Effect of Length of Boom Support Leg on Free Standing Jib Crane", *International Journal of Scientific Engineering and Research (IJSER)*, ISSN 2319-7064, Volume 4, Issue 5, pp. 19-23, (2016)
- [8] Gening Xu, Guangheng Gao, "Displacement Calculation Method of Super-long Telescopic Jib Structure Considering the Effect of Self Weight and Large Deformation", *Researches and Applications in Mechanical Engineering Vol. 2*, Issue 4, ISSN 2327-1582, pp. 99-104, (2013)
- [9] Kiranalli S.S., Patil N.U., "Jib Crane Analysis using FEM", *IJSRD - International Journal for Scientific Research & Development*, ISSN (online): 2321-0613 Volume 3, Issue 4, pp. 185-189, (2015)
- [10] Khetre S.N., Chaphalkar S. P., Meshram A., "Modelling and stress analysis of column bracket for rotary jib crane", *International Journal of Mechanical Engineering and Technology (IJMET)*, ISSN 0976-6359, Volume 5, Issue 11, pp. 130-139, (2014)
- [11] Gašić V., Zrnić N., Rakin M., "Consideration of a moving mass effect on dynamic behaviour of a jib crane structure", *Technical Gazette*, ISSN 1848-6339, Volume 19, Issue 1, pp. 115-121, (2012)
- [12] Ma, Xiao, and Hui Wang. "Column Jib Crane Based on ANSYS Analysis of Static Stiffness and Improving Measures." *Key Engineering Materials*, ISSN 1662-9795, Vol. 522, pp. 485–89, (2012)
- [13] Pavlović G., Gašić M., Savković M., Zdravković N., Marković G., "Comparative analysis of the models for determination of deflection in the column-mounted jib crane structure", *Mechanics Transport Communications*, ISSN 2367-6620, Vol. 15, No. 3/2, pp. V-5-V11, (2017)
- [14] Nebojša Zdravković, Mile Savković, Goran Marković, Goran Pavlović, "The determination of the deflection of the beam with continuously varying cross-section by the finite difference method", *IMK-14 – Research & Development in Heavy Machinery*, Vol. 26, No. 1, ISSN 0354-6829, pp. EN19-EN 23, (2020)
- [15] <https://jibcranemanufacturer.com/pillar-jib-crane>